Cite this: DOI: 10.1039/c0xx00000x

www.rsc.org/xxxxxx

ARTICLE TYPE

Mechanistic insights into catalytic oxidations of organic compounds by ruthenium(IV)-oxo complexes with pyridylamine ligands

Shingo Ohzu,[a] Tomoya Ishizuka,[a] Yuichirou Hirai,[b] Hua Jiang,[a] Miyuki Sakaguchi,[c] Takashi Ogura,[c] Shunichi Fukuzumi,*[b,d] and Takahiko Kojima*[a]

Received (in XXX, XXX) Xth XXXXXXXXX 20XX, Accepted Xth XXXXXXXXX 20XX

DOI: 10.1039/b000000x

A series of Ru(IV)-oxo complexes (**4**–**6**) were synthesized from the corresponding Ru(II)-aqua complexes (**1**–**3**) and fully characterized by ^{1}H NMR and resonance Raman spectroscopies, and ESI-MS spectrometry. Based on the diamagnetic character confirmed by the ^{1}H NMR spectroscopy in D_2O, the spin states of **5** and **6** were determined to be $S = 0$ in the d^4 configuration, in sharp contrast to that of **4** being in the $S = 1$ spin state. The aqua-complexes **1**–**3** catalyzed oxidation of alcohols and olefins using $(NH_4)_2[Ce^{IV}(NO_3)_6]$ (CAN) as an electron-transfer oxidant in acidic aqueous solutions. Comparison of the reactivity of electrochemically-generated oxo-complexes (**4**–**6**) was made in the light of kinetic analyses for oxidation of 1-propanol and a water-soluble ethylbenzene derivative. The oxo complexes (**4**–**6**) exhibited no significant difference in the reactivity for the oxidation reactions, judging from the similar catalytic rates and the activation parameters. The slight difference observed in the reaction rates can be accounted by the difference in the reduction potentials of the oxo-complexes, but the spin states of the oxo-complexes have hardly affected the reactivity. The activation parameters and the kinetic isotope effects (KIE) observed for the oxidation reactions of methanol indicate that the oxidation reactions of alcohols with the Ru^{IV}=O complexes proceed *via* a concerted proton-coupled electron transfer mechanism.

Introduction

High-valent metal-oxo complexes are one of the most important classes of compounds because of their indispensable roles as reactive intermediates in a number of biological and chemical oxidation reactions.[1-3] Therefore, formation and reactivity of high-valent metal-oxo complexes and the reaction mechanisms have been intensively investigated for these decades.[4-10] One of the major procedures to form high-valent metal-oxo complexes is proton-coupled electron-transfer (PCET) oxidation of metal-aqua complexes using water as an oxygen source of the oxo ligand.[11,12] The PCET pathway plays an important role in the oxygen-evolving complex (OEC) in photosystem II.[13,14] OEC consists of a tetranuclear Mn-oxo cluster residing at the reaction center and the cluster catalyzes four-electron oxidation of water to evolve molecular oxygen. It has been proposed that an aqua-ligated manganese site in the cluster is oxidized to generate a Mn^V=O species via a PCET process and the resulting Mn^V=O to species acts as a reactive intermediate to oxidize a water molecule give molecular oxygen.[13]

Meyer and co-workers have developed catalytic water-oxidation systems using $Ru(OH_2)$-polypyridyl complexes[11] and mechanisms of catalytic water-oxidation systems using Ru^V=O complexes produced via PCET reactions with one-electron oxidants have been extensively studied.[15-18] In addition, Ru^{IV}=O complexes, which are formed by PCET oxidations of corresponding Ru(II)-aqua precursor complexes, have also been intensively investigated to gain mechanistic insights into the oxidation reactions of organic substrates.[19] However, as far as we know, few catalytic oxidation systems for organic substrates have been reported, including PCET processes to generate an active metal-oxo species.[12b] Recently, we have reported catalytic oxidation systems, where a PCET oxidant was employed to oxidize Ru^{II}-OH_2 complexes (**1** and **2**) to form the corresponding reactive Ru^{IV}=O complexes (**4** and **5**) and organic substrates such as alcohols and olefins were catalytically oxidized with high

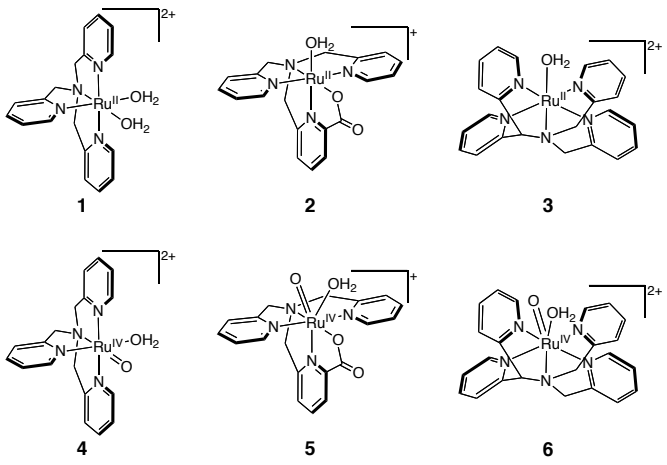

Fig. 1 Molecular structures of high-valent Ru(IV)=O complexes.

efficiency to give a single oxidized product from a substrate.[20, 21]

We report herein a novel Ru^{II}-OH_2 complex (**3**) with a pentadentate N4Py ligand (N4Py = *N*,*N*-bis(2-pyridyl-methyl)-*N*-bis(2-pyridyl)methylamine)[22] as a candidate for an oxidation catalyst of organic substrates. We have also prepared a new Ru(IV)=O complex (**6**) in an $S = 0$ spin state.[20b] Including the former Ru^{II}-OH_2 complexes (**1** and **2**), are available three different precursor complexes with similar ancillary ligands as tris(2-pyridylmethyl)amine (TPA) derivatives. Those precursor complexes can be oxidized to afford corresponding Ru^{IV}=O species exhibiting different reduction potentials and different spin states. Therefore, by preparing the three different Ru(IV)=O complexes (**4**–**6** in Fig. 1), we can investigate the details on the influence of difference of spin states of Ru^{IV}=O complexes on the reactivity together with mechanistic insights into oxidation of organic substrates on the basis of kinetic analysis. In addition, we examined the effect of the reduction potentials of the active metal-oxo species on the PCET reactivity.

Results and Discussion

Molecular design and synthesis

Herein, we have prepared three kinds of ruthenium(II)-aqua complexes (**1**–**3** in Fig. 1), which have TPA and its derivatives, 2-(6-carboxyl-pyridyl)methyl-bis(2-pyridylmethyl)amine (6-COOH-TPA)[22] and N4Py as ligands. As we reported previously, the Ru^{IV}=O complex with TPA (**4**) was revealed to be in the $S = 1$ spin state in water,[20a] whereas the Ru^{IV}=O complex with 6-COO^--TPA (**5**) showed the unprecedented spin state, $S = 0$, in water.[20b] One of the main reasons that the complex **5** shows such an unusual spin state for Ru^{IV} complexes is the distorted coordination environment of 6-COO^--TPA: The distorted coordination environment allowed the additional coordination of a water molecule to the Ru center to afford a seven-coordinated and pentagonal bipyramidal structure. The coordinated water molecule enabled the complex to form hydrogen bonding between water molecules of the solvent. The seven-coordinate environment has been suggested to stabilize the diamagnetic $S = 0$ spin state of the Ru(IV)-oxo complex compared to the paramagnetic $S = 1$ spin state.[20b] Therefore, we have employed another pentadentate TPA derivative, N4Py, as a ligand in this work to attain a distorted coordination environment[22] for achieving a seven-coordinate structure in water.

The synthesis of a Ru(II)-aqua complex of N4Py, $[Ru^{II}(N4Py)(OH_2)](PF_6)_2$ (**3**), was accomplished by the treatment of $[Ru^{II}Cl(N4Py)](PF_6)$[24] with $AgPF_6$ (Scheme 1). Full characterization of **3** was made by ^1H NMR spectroscopy, ESI-TOF-MS spectrometry, elemental analysis, and X-ray diffraction analysis (*vide infra*). The aqua-complex **3** was oxidized into the Ru(IV)-oxo complex, $[Ru^{IV}(O)(N4Py)(OH_2)](PF_6)_2$ (**6**), with $(NH_4)_2$-$Ce^{IV}(NO_3)_6$ (CAN) as an oxidant. The characterization of **6** was performed by using ^1H NMR and resonance Raman spectroscopies and also by ESI-TOF-MS spectrometry (*vide infra*).

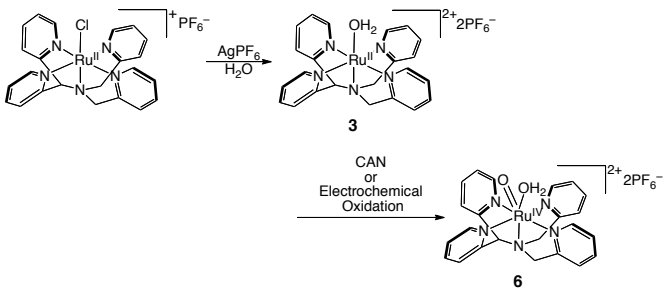

Scheme 1 Synthesis of $[Ru^{IV}(O)(N4Py)](PF_6)_2$ (**6**).

Crystal structure of 3

A single crystal of **3** suitable for X-ray crystallography was obtained by vapor diffusion of octane into the CH_2Cl_2 solution. An ORTEP drawing of the cation part of **3** is depicted in Fig. 2. Complex **3** was crystallized into a *monoclinic* lattice with the space group of $P2_1/n$: The asymmetric unit consisted of the cationic part of **3**, $[Ru^{II}(N4Py)(OH_2)]^{2+}$, two PF_6^- ions as counter anions, and a CH_2Cl_2 molecule as a solvent molecule of crystallization. One of the two PF_6^- ions and a half of the co-crystallized CH_2Cl_2 molecule were overlapped on one position by disorder. The bond lengths between the central Ru(II) ion and the pyridine nitrogen atoms of N4Py are in a normal range,[25] however, that of Ru-N1 (tertiary amino nitrogen) is relatively shorter as compared to other Ru-N*x* (x = 2~5) distances: The short bond between Ru and N1 should be derived from the strong σ-donation of the tertiary amine properties of N1. The bond length of Ru-O1 (2.172(5) Å) was slightly longer than those reported so far for Ru^{II}-OH_2 (2.10–2.14 Å).[26] The number of the counter anions and the bond distances around the Ru center strongly indicate that the oxidation state of the Ru center should be +2. The Ru center was positioned in mean planes consisting of O1-N1-N2-N4 and O1-N1-N3-N5 with the deviations from the planes to be 0.024 and 0.021 Å, respectively. On the other hand, the Ru center is largely deviated from the mean plane consisting of N2-N3-N4-N5 to the opposite direction of N1 with the distance of 0.263 Å. This deviation was also related to the fact that all the bond angles of N1-Ru-N*x* (x = 2~5) for five-membered chelate rings are smaller than 90° (Table S1 in Electronic Supplementary Information (ESI)) and that the bond angles of N2-Ru-N4 (165.38(18)°) and N3-Ru-N5 (165.14(19)°) are both much smaller than 180°. In addition, a trend was

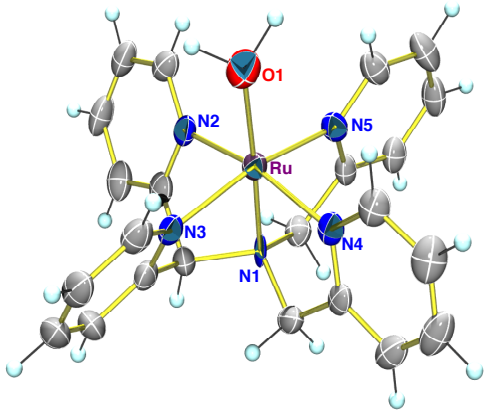

Fig. 2 Crystal structure of the cation part of **3**. Each atom is described with a thermal ellipsoid at 50% probability. Selected bond lengths (Å); Ru-O1: 2.172(5), Ru-N1: 1.967(5), Ru-N2: 2.057(4), Ru-N3: 2.052(4), 2.061(4), Ru-N5: 2.060(5), and angle(°); O1-Ru-N1: 177.63(18).

observed that the pyridine rings bonded to the methine carbon of the N4Py ligand (pyridine rings containing N2 and N3) were largely tilted relative to an equatorial plane compared to the pyridine rings bonded to the methylene carbons (pyridine rings containing N4 and N5). The dihedral angles between the O1-N1-N2-N4 plane and the N2- and N4-pyridine rings were 30.5° and 13.5°, respectively, and those between the O1-N1-N3-N5 plane and the N3- and N5-pyridine rings were 51.4° and 12.4°, respectively. The tilting may disturb the efficient π-back donation from the Ru center to the pyridine rings. As a result of the distortion of the coordination environment around the Ru center, the Lewis acidity of the Ru center should increase.

Spectroscopic and electrochemical characterization of 3

The spectroscopic titration of complex **3** was performed in Britton-Robinson (B.-R.) buffer[27] by addition of a 10 M NaOH aqueous solution using absorption spectroscopy. On the basis of the absorbance changes, the pK_a values of the aqua ligand in **3** were determined as shown in Fig. S1 in ESI. The pK_{a1} value for the first deprotonation of the aqua ligand was determined to be 1.85±0.02 and the pK_{a2} value for the deprotonation of the hydroxo-ligand was determined to be 12.0±0.1. The pH-dependent absorption spectral changes were reversible. For comparison, spectroscopic and electrochemical data of the Ru(II)-aqua and Ru(IV)-oxo complexes are summarized in Table 1.

Cyclic and differential-pulse voltammograms (CV and DPV, respectively) of **3** were also measured in B.-R. buffer at various pH (Fig. S2 in ESI) and the Pourbaix diagram was drawn based on the results of the electrochemical measurements and the pK_a values obtained (Fig. 3). Above pH 1.8, the aqua ligand of **3** should be deprotonated on the basis of the pK_{a1} value, and thus, the initial state of the complex for the electrochemical measurements is $[Ru^{II}(OH)(N4Py)](PF_6)$ (Ru^{II}-OH^-). In the Pourbaix diagram, the potential of the first oxidation step is constant to be +0.55 V *vs.* SCE up to pH 2.5, and in the pH range over 2.5, it decreases as the solution pH increases with an inclination of –0.054 V/pH, indicating the 1 e^- and 1 H^+ process of the Ru^{II}-OH^- complex to give $[Ru^{III}(O)(N4Py)]^+$ (Ru^{III}-O^{2-}). Therefore, the p*K*a value of $[Ru^{III}(OH)(N4Py)]^{2+}$ was estimated to be 2.5. The potential of the second one-electron oxidation step decreased up to pH 2.5 with an inclination of –0.055 V/pH, which was ascribed to a proton-coupled process of Ru^{III}-OH^- → $[Ru^{IV}(O)(N4Py)]^+$ (Ru^{IV}=O). Above pH 2.5, the second oxidation potential was determined to be constant (+0.87 V *vs*. SCE), independent on the pH value and thus, the process can be ascribed to the change from Ru^{III}-O^{2-} to Ru^{IV}=O. The one-electron reduction potential (+0.90 V *vs*. SCE) of the Ru^{IV}=O species at pH 2 is higher than those of **1** (+0.75 V)[20a] and **2** (+0.68 V),[20b] allowing us to expect higher reactivity of **3** for oxidation reactions as compared to those of complexes **1** and **2** (*vide infra*).

Electrochemical oxidation of the aqua complexes **1**–**3** at +1.3 V (*vs*. SCE) in B.-R. buffer clearly indicated the two-step spectral changes due to generation of the corresponding Ru(III) complexes and the Ru(IV)-oxo complexes with clear isosbestic points (Fig. 4). The reactions were completed in 1 h. In the case of **1**, the electrochemical oxidation for the first 30 min gave rise to the spectral change with two isosbestic points at 565 and 256 nm and a new broad absorption band around 500 nm, as shown in Fig. 4a. For the next 30 min, the isosbestic point was shifted to 294 nm and a new broad band appeared at 410 nm (Fig. S3 in ESI). As for the complex **2**, the spectral change for the first 30 min proceeded with an isosbestic point at 600 nm to give a new broad absorption at λ_{max} = 548 nm as depicted in Fig. 4b. The isosbestic point for the spectral changes of **2** during the next 30 min was observed at 287 nm (Fig. S3b in ESI). As the oxidation of **3** proceeded, the MLCT absorption at 440 nm gradually faded and instead a new broad absorption was observed at 260-300 nm (Fig. 4c). For the first 30 min, two isosbestic points appeared at 325 and 258 nm, and during the next 30 min, no isosbestic point was observed within the wavelength range measured. The absorption spectral changes in the course of the electrochemical oxidations of complexes **1**–**3** ended at the elementary electric charges of 0.198 C for **1**, 0.201 C for **2**, and 0.188 C for **3**, loaded into the solution, which are comparable to the theoretical value for the two-electron oxidation of Ru^{II} species to form the corresponding Ru^{IV} complexes (0.193 C).

ESI-MS spectrum was measured for the aqueous solution of **6** generated by the oxidation with CAN and a peak cluster was

Table 1. Summary of the analytical data for **1**, **2** and **3**.

	1[d]	**2**[e]	**3**
pK_{a1} [a]	2.1	3.5	1.85±0.02
pK_{a2} [a]	8.5	—	12.0±0.1
$E_{1/2}$ ($Ru^{II/III}$, V *vs*. SCE) at pH 1.8 [b]	+0.48	+0.40	+0.60
$E_{1/2}$ ($Ru^{III/IV}$, V *vs*. SCE) at pH 1.8 [b]	+0.75	+0.68	+0.87
ν (Ru=^{16}O) [cm^{-1}] [c]	806	833	801
ν (Ru=^{18}O)[cm^{-1}] [c]	764	788	761
$\Delta\nu$ (^{16}O – ^{18}O) [cm^{-1}]	42	45	40

[a] 0.1 M solution in B.-R. buffer titrated with a 10 M NaOH aqueous solution at room temperature. [b] 0.1 mM solution in B.-R. buffer at room temperature; scan rate: 0.1 V/s. [c] Data obtained by resonance Raman spectroscopy. [d] ref. 24a. [e] ref. 24b.

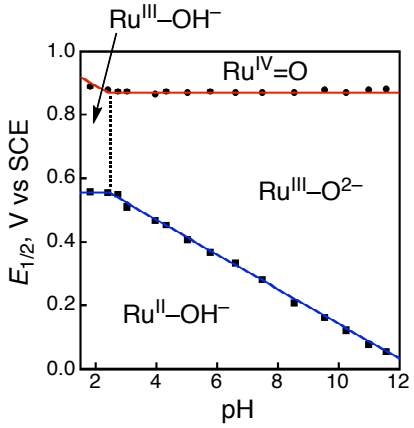

Fig. 3 A plot of redox potentials against solution pH (Pourbaix diagram) for complex **3** in a B.-R. buffer. Potentials were determined relative to SCE (as 0 V) at room temperature. The squares and blue line indicate the $Ru^{II/III}$ couples, and the circles and red line correspond to the $Ru^{III/IV}$ couples.

observed at m/z = 242.56 with the feature of a divalent cation, which was ascribable to the signal of $[\mathbf{6} - 2PF_6]^{2+}$ (Fig. S4 & Fig. S5 in ESI). When the oxidation of **3** was performed in $H_2{}^{18}O$, the peak cluster was shifted to m/z = 243.54 assigned to ^{18}O-labeled $[Ru^{IV}(^{18}O)(N4Py)]^{2+}$ (*calcd.* 243.54) (Fig. S4b in ESI) via the substitution of the ^{16}O-aqua ligand with $H_2{}^{18}O$.[28] The ESI-MS spectrum of the complex **6** generated electrochemically displayed the same features with those for the sample obtained by the oxidation of **3** with CAN (Fig. S6 in ESI).

Resonance Raman spectroscopy suggests the existence of a Ru=O double bond in **6** (ν = 801 cm^{-1}) and the Raman scattering band was shifted to ν = 761 cm^{-1} with the use of $H_2{}^{18}O$ in place of $H_2{}^{16}O$ as the solvent for the formation of the Ru(IV)-oxo complex (Fig. S7 in ESI).[29] The observed isotope shift ($\Delta\nu$ = 40 cm^{-1}) showed a good agreement with the calculated value ($\Delta\nu$ = 40 cm^{-1}) for the Ru=O harmonic oscillator.[20] The Raman shift of the Ru^{IV}=O bond for **6** is comparable to those of **4** with TPA (806 cm^{-1})[20a] and $[Ru(O)(TPA)(bpy)]^{2+}$ (805 cm^{-1}),[30] but lower than that (833 cm^{-1}) of **5** with 6-COO^--TPA.[20b]

The ^{1}H NMR spectrum of **6** generated by the oxidation of **3** with CAN[31] in D_2O showed well-resolved signals in the range of

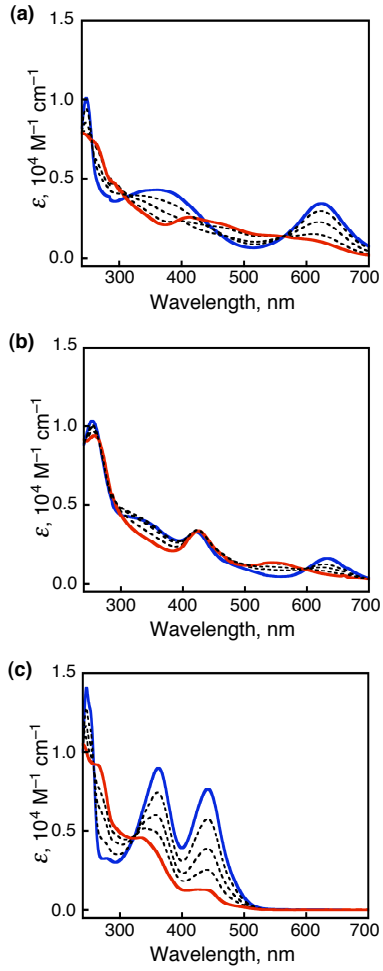

Fig. 4 Spectral changes of every 15 min during the electrochemical oxidation of (a) **1**, (b) **2**, and (c) **3** in B.-R. buffer (pH 1.8; sample concentration, 0.5 mM) at room temperature. The initial spectrum of each complex and the final spectrum are indicated as the blue and red lines, respectively.

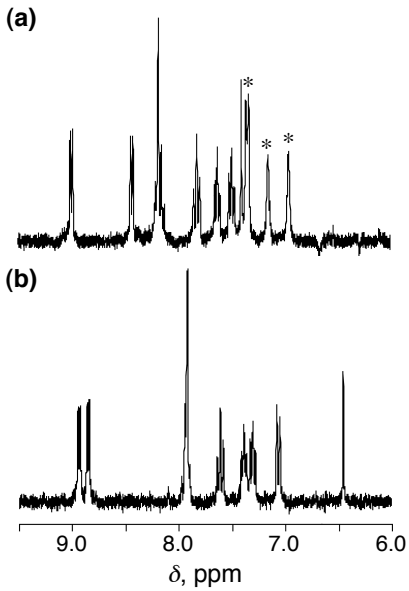

Fig. 5 ^{1}H NMR spectra of complex a) **6** and b) **3** in D_2O. The asterisks (*) denote signals derived from ammonium ion of CAN.

3 – 9 ppm, indicating a diamagnetic character of **6**, and thus, the spin state of **6** is obviously S = 0 (Fig. 5) at room temperature. In addition, the yield of **6** based on the amount of **3** was nearly quantitative, as estimated by peak integration of the ^{1}H NMR signals relative to that of DSS (= 4,4-dimethyl-4-silapentane-1-sulfonic acid) added as an internal reference. The assignment of the ^{1}H NMR signals due to both of **3** and **6** were performed with 2D ^{1}H-^{1}H COSY and 1D NOE measurements (Fig. S9 and S10 in ESI). In comparison of the spectrum of complex **6** in D_2O with that of **3**, most of the ^{1}H NMR signals of **6** exhibited down-field shifts due to the higher oxidation state of the Ru(IV) center in **6** than those of **3** with Ru(II), and thus, the Lewis acidity of the Ru center should be enhanced in **6** to exert stronger electron-withdrawing effects on the ligand. Characteristic differences in the ^{1}H NMR spectra between **3** and **6** were observed for the signals of 6-Hs of the pyridine rings bonded to the methylene carbon (doublet), the proton of the methine carbon (singlet), and the methylene protons (AB quartet); the shift widths ($\Delta\delta$) for the proton signals from complex **6** to **3** were –0.40, +0.97, +0.95 and +1.24 ppm, respectively. The large downfield shifts of the methine- and methylene-protons may be ascribed to the effect of the increase in the oxidation number at the Ru center as a Lewis acid, affecting most strongly the σ-donating amine nitrogen (N1) of the N4Py ligand through the strong σ-bond between them. The effect of oxidation of the Ru center also strongly influences the electronic states of the carbons adjacent to the amine nitrogen. The upfield shifts of 6-Hs of the pyridine rings bonded to the methylene carbon (N4- and N5-pyridine rings)[32] is probably ascribed to the tilt of the pyridine rings, which is caused by the steric effect of the additional coordination of a water molecule (*vide infra*). As a result of the tilting, the 6-Hs are located on the ring currents of the pyridine rings bonded to the methine carbons (N2- and N3-pyridine rings).

Origins of the unusual S = 0 spin state for Ru^{IV}=O species 5 and 6

We have reported that a seven-coordinated pentagonal bipyramidal structure of the Ru center involving an additional aqua ligand derived from the solvent, as suggested by DFT calculations on **5** with 6-COO^--TPA, plays a key role to stabilize the singlet state relative to the triplet state in water.[20b] In the case of **6**, a seven-coordinated structure with a solvent water molecule, as well as in the case of **5**,[20b] is indispensable to stabilize $S = 0$ state of **6** (Fig. 6), since the coordination environment made of the N4Py ligand is distorted from an ideal octrahedron as seen in the crystal structure of **3**. As a result of the seven coordination, the total electron density donated from the ligands in the basal equatorial plane of the pentagonal bipyramid increased and the d_{xy} orbital of the Ru(IV) center is destabilized and the singlet state becomes more favored than the triplet state. Thus the formulation of low-spin **6** should be $[Ru(O)(N4Py)(OH_2)]^{2+}$ in water.

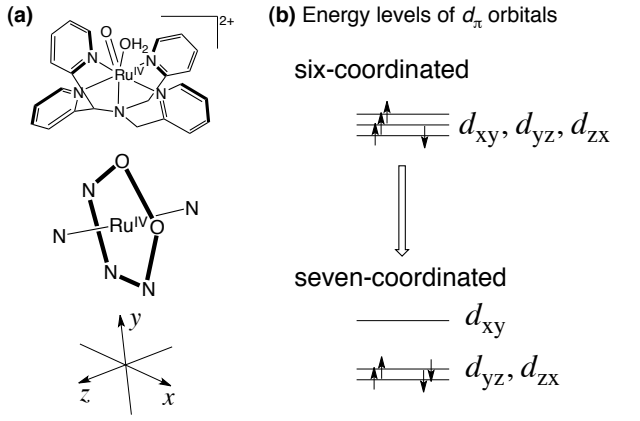

Fig. 6 (a) Schematic description of a seven-coordinated structure of **6** and (b) the effect of the seven coordination on the energy levels of the d_π orbitals.

Catalytic oxidation of organic substrates

By using the Ru(II)-aqua complexes, $[Ru^{II}(TPA)(OH_2)_2](PF_6)_2$ (**1**), $[Ru^{II}(6\text{-}COO\text{-}TPA)(OH_2)](PF_6)$ (**2**) and complex **3** as catalysts, catalytic oxidation reactions of benzyl alcohol and the *para*-substituted derivatives, aliphatic alcohols (1- and 2-propanols, and methanol), olefins (styrene and cyclohexene) and a water-soluble ethylbenzene derivative were carried out with CAN as an electron-transfer oxidant in D_2O at room temperature. The product yields after stirring for 1 h were determined by ^1H NMR spectroscopy (Table 2 and Fig. S11 in ESI). As control experiments, we examined the reactions of the substrates listed in Table 2 with CAN under the same reaction conditions except the absence of the catalysts to confirm that the substrates employed were almost intact and persistent against CAN under the reaction conditions.[33]

In the case of oxidation of benzyl alcohol derivatives, the two-electron oxidation occurred to give the corresponding aldehydes for primary alcohols (entries 1–4) and ketone for a secondary alcohol (entry 5). 1-Propanol underwent the four-electron oxidation to afford propionic acid (entry 6) and 2-propanol was converted to acetone via the two-electron oxidation (entry 7). Methanol with the C-H bond dissociation energy of 96.0 kcal mol^{-1} [34] could be oxidized to afford formaldehyde through the two-electron oxidation (entry 8). Terminal and internal alkenes

Table 2 Summary of turnover numbers and the oxidation efficiency (%) of the catalytic oxidation reactions with **1**–**3** as catalysts[a].

			turnover number (efficiency, %)[b] catalyst		
entry	substrate	product	**1**	**2**	**3**
1	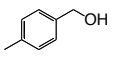	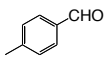	100 (100)	100 (100)	100 (100)
2	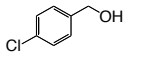	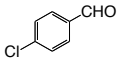	100 (100)	98 (98)	95 (95)
3	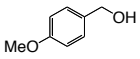	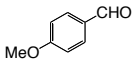	98 (98)	96 (96)	91 (91)
4	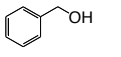		93 (93)	91 (91)	90 (90)
5	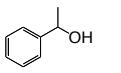		90 (90)	88 (88)	85 (85)
6	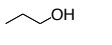		50 (100)	47 (94)	42 (84)
7			100 (100)	98 (98)	82 (82)
8	CH_3OH	HCHO	25 (25)	23 (23)	22 (22)
9	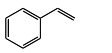		46 (92)	42 (84)	39 (78)
10		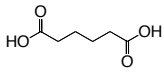	25 (100)	23 (92)	9 (36)
11	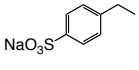	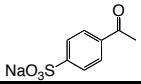	38 (76)	35 (70)	33 (66)

[a] [substrate] = 0.1 M, [CAN] = 0.2 M, [catalyst] = 1 mM. [b] Turnover number = [Product]/[catalyst]; efficiency (%) = [product]·n/[CAN] (n: number of electrons related to the oxidation).

underwent oxidative C=C bond cleavage; styrene was converted to benzaldehyde (entry 9) and cyclohexene to adipic acid via an eight-electron oxidation (entry 10). A water-soluble ethylbenzene derivative was also converted to afford the acetophenone derivative via a four-electron oxidation (entry 11).

The oxidation efficiency for alcohols except methanol is nearly 100% in common with all the three catalysts. On the other hand, the oxidation of olefins with catalyst **3** exhibited relatively low efficiencies compared to the catalysts **1** and **2**. The reason for the low efficiency is probably due to the difference in the stability among the three catalysts: The catalyst **1** is remarkably robust under catalytic conditions and alive even after more than 2500 catalytic cycles,[20a] whereas the catalyst **3** was not so stable and gradually decomposed under the same catalytic reaction conditions. Therefore, the oxidation of olefins, the rates of which were relatively slow as compared to those of alcohols, could not be completed by **3** because the catalyst **3** decomposed before the completion of the reaction.

Kinetic studies under pseudo-first-order conditions

In order to reveal the reaction mechanisms of the oxidation of organic substrates with Ru(IV)-oxo complexes **4**–**6** and also to

compare the reactivity among the three Ru(IV)-oxo complexes in the light of the difference of the spin states, we performed the kinetic analyses on the quantitative oxidation of 1-propanol with electrochemically generated Ru^{IV}=O species **4**–**6**. The reactions were performed in the presence of an excess amount of 1-propanol (25–150 mM) relative to the Ru^{IV}=O species (0.5 mM) in B.-R. buffer and the rate constants were determined by monitoring absorbance changes at 624 nm for **4**, 628 nm for **5** and 440 nm for **6** at various temperatures (Fig. S13 in ESI). All the time courses of the absorbance changes obeyed first-order kinetics and the pseudo-first-order rate constants were determined with various concentrations of 1-propanol (Fig. 7 and Fig. S14 in ESI). In the oxidation of 1-propanol with **4**–**6**, saturation behaviors of the pseudo-first-order rate constants (k_{obs}) with respect to concentration of 1-propanol were commonly observed for **4**–**6** at all the temperatures examined, indicating the existence of pre-equilibrium processes prior to the oxidation. Hence, non-covalent interaction between 1-propanol and **4**–**6** results in formation of the corresponding precursor complexes. The curve fitting to the plots of k_{obs} relative to concentration of the substrate with Eq. (1) gave the equilibrium constants (K) of

$$k_{obs} = kK[\text{1-propanol}]/(1 + K[\text{1-propanol}]) \quad (1)$$

the pre-equilibrium process and the rate constants (k) of the oxidation reactions[35] and those values obtained at various temperatures are summarized in Table 3. The plots of the equilibrium constants K and the rate constants k relative to inverse of the reaction temperatures (T^{-1}) (van't Hoff plots and Eyring plots, respectively; see Fig. S15 in ESI) allowed us to obtain the thermodynamic parameters for the pre-equilibrium processes and the activation parameters for the oxidation reactions, respectively (Table 3).[36]

As indicated by the thermodynamic parameters for the pre-equilibrium processes (ΔH and ΔS), the formation of the precursor complexes is exothermic and the order of the ΔH values suggests that the interaction between 1-propanol and the Ru^{IV}=O complexes can be ascribed to the hydrogen bonding. In the hydrogen bonding, the aqua ligand of **4** and the additional aqua ligands of **5** and **6** affording a seven-coordination environment should play an important role to stabilize the adduct between the oxo complexes and the substrate (*vide supra*). The activation parameters determined from the Eyring plots shed lights on the

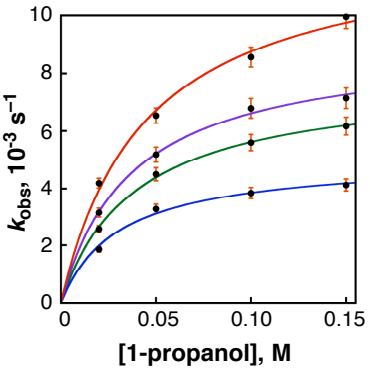

Fig. 7 Pseudo-first-order kinetic analysis for oxidation of 1-propanol with complex **6** as oxidants (0.5 mM) in B.-R. buffer (pH 1.8) at 308 (red), 301 (purple), 288 (green), and 280 K (blue).

transition states of the oxidation reactions and provided some fundamentals to consider the difference in the reactivity of **4**–**6**. The activation parameters obtained here for oxidants **4**–**6** are similar to each other, indicating that the reaction proceeds via similar transition states for the three oxidants in terms of energies and structures. In addition, the negatively large activation entropies suggest the tight interaction between the substrate and the oxidants during the dehydrogenation processes (*vide infra*).

The kinetic analysis was also conducted for the oxidation of sodium 4-ethylbenzene-sulfonate (EBS) with oxidants **4**–**6** in water at 295 K. Unexpectedly, the pseudo-first-order rate constants (k_{obs}) exhibited saturation behaviors relative to the concentration of EBS, which has no hydroxy group, in common for all the three oxidants (Fig. S16 in ESI). The obtained pre-equilibrium constants and the rate constants for the oxidation of EBS at 295 K with **4**–**6** are summarized in Table 3c. The equilibrium constants of the precursor complex formation between the oxidant and the substrate in the oxidation of EBS are smaller than those for the oxidation of 1-propanol, whereas the rate constants of the former are larger than the latter. As EBS does not possess any strong hydrogen-bonding sites, the pre-equilibrium processes are possibly derived from weak non-covalent interaction between the substrate and the oxidants such as non-classical hydrogen bonding between the rather basic

Table 3 Kinetic data for oxidation reactions with complexes **4**–**6**. (a) equilibrium constants of adduct formation between the oxidant and 1-propanol and the thermodynamic parameters; (b) pseudo-first-order rate constants and the activation parameters for oxidation of 1-propanol at various temperatures; (c) equilibrium constants of the adduct formation and pseudo-first-order rate constants for oxidation of sodium 4-ethylbenzene sulphonate at 295 K.

(a)

	4	**5**	**6**
K_{308K} [M^{-1}]	32±5	27±2	22±3
K_{301K} [M^{-1}]	36±5	41±2	28±2
K_{288K} [M^{-1}]	53±3	61±7	31±2
K_{280K} [M^{-1}]	92±6	92±4	45±5
ΔH [kJ mol^{-1}]	-23.8±0.2	-29.7±0.3	-16.2±0.8
ΔS [J K^{-1} mol^{-1}]	-4.8±0.3	-6.8±0.2	-2.6±0.1

(b)

	4	**5**	**6**
k_{308K} [10^{-3} s^{-1}]	9.3±0.4	8.2±0.2	12.4±0.5
k_{301K} [10^{-3} s^{-1}]	6.9±0.3	5.2±0.5	9.0±0.2
k_{288K} [10^{-3} s^{-1}]	4.6±0.3	3.7±0.1	7.8±0.2
k_{280K} [10^{-3} s^{-1}]	2.9±0.5	2.6±0.1	5.0±0.2
$\Delta H^{\ddagger}$ [kJ mol^{-1}]	25.6±0.4	22.0±0.2	17.5±0.8
$\Delta S^{\ddagger}$ [J K^{-1} mol^{-1}]	–201±3	–215±2	–225±10

(c)

	4	**5**	**6**
K_{295K} [M^{-1}]	7.8±1.0	7.8±1.3	7.8±1.9
k_{295K} [10^{-3} s^{-1}]	17.7±1.0	15.8±1.2	15±2

oxo ligand and the substrate C-H bond.[37] In addition, the larger rate constants for the oxidation of EBS compared to those for the oxidation of 1-propanol can be ascribed to the feasibility of the hydrogen atom abstraction from EBS than that from 1-propanol as can be predicted from the values of bond dissociation energies (BDEs) of C-H bonds: 84.6 kcal/mol for ethylbenzene and 93.7 kcal/mol for 1-propanol.[34]

Kinetic isotope effects on the oxidation of methanol

In order to obtain the further information on the oxidation process, studies of the kinetic isotope effects (KIE) with the three Ru^{IV}=O complexes were conducted for the oxidation of methanol at 297 K. The KIE values were determined as the ratio of the rate constants (k_H/k_D) for the oxidation reactions of CH_3OH and deuterated methanol derivatives (Fig. 8 & Fig. S17 in ESI). The oxidation of CH_3OH was performed in water in the presence of one of the three oxidants (**4**–**6**) (0.5 mM). CD_3OH was formed in situ by addition of CD_3OD (deuteration percentage: 99.8%) into the solution of one of the three oxidants in H_2O. The oxidation of CH_3OD with one of the three oxidants was performed in a D_2O solution of CH_3OH (deuteration percentage: 99.9%). The reactions were monitored by UV-Vis spectroscopy to track the rise of the absorbance due to the Ru^{II} species formed.

The pseudo-first-order rate constants for the methanol oxidation also displayed saturation behaviors as in the cases of 1-propanol and EBS as described above. The equilibrium constants and the first-order rate constants are summarized in Table 4. The pre-equilibrium constants are larger in the cases of oxidation of CD_3OH in comparison with those of CH_3OH for all the three oxidants; however, those for CH_3OD were comparable to those for CH_3OH. The KIE values for the hydroxy group, which were determined by using CH_3OH and CH_3OD as substrates, were negligible for the three oxidants to be 1.0 for **4** and 1.1 for **5** and **6** (Table 4). In contrast, the oxidation of CD_3OH was clearly retarded as compared to that of CH_3OH to show KIE values to be 2.5 for **4**, 2.3 for **5**, and 1.7 for **6** (Table 4). The KIE values of CH_3OD *vs*. CD_3OH indicate that the hydrogen abstraction from the methyl group is involved in the rate-determining step, however, the hydrogen abstraction from the OH group is not

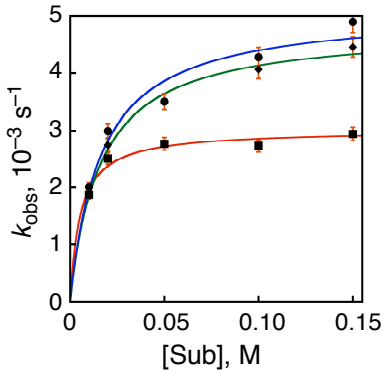

Fig. 8 Pseudo-first-order kinetic analysis for oxidation reactions of CH_3OH (blue line), CD_3OH (red line) and CH_3OD (green line) with complex **6** as oxidants at 297 K. CH_3OH and the deuterated derivatives (CD_3OH and CH_3OD) were used as substrates.

Table 4. Rate constants and equilibrium constants for oxidation of methanol with **4**–**6** at 297 K.

	4	**5**	**6**
k_{CH3OH} [10^{-3} s^{-1}]	5.0±0.3	4.5±0.3	5.1±0.3
K_{CH3OH} [M^{-1}]	44±6	43±7	62±15
k_{CD3OH} [10^{-3} s^{-1}]	2.0±0.6	2.0±1.0	3.0±0.1
K_{CD3OH} [M^{-1}]	43±4	47±9	96±19
k_{CH3OD} [10^{-3} s^{-1}]	5.0±0.3	4.1±0.2	4.8±0.1
K_{CH3OD} [M^{-1}]	32±3	41±5	63±7
k_H/k_D for CH_3	2.5	2.3	1.7
k_H/k_D for OH	1.0	1.1	1.1

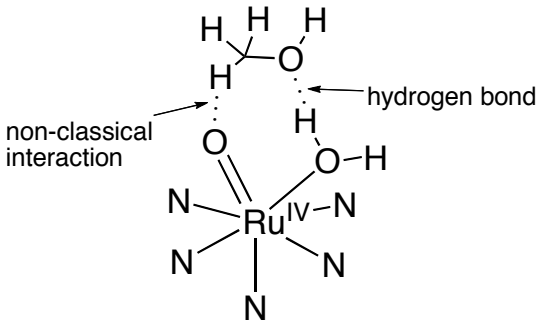

Fig. 9 Plausible hydrogen bonding between seven-coordinate Ru^{IV}=O complexes with an aqua ligand and methanol.

involved in the rate-determining step.

The α-C–H bond in a hydrogen-bonded alcohol can be oriented to the oxo ligand to undergo hydrogen atom abstraction to give rise to a tightly condensed transition state, as reflected on the negatively large entropy ($\Delta S^{\ddagger}$), –201±3 J K^{-1} mol^{-1} for **4**, –215±2 J K^{-1} mol^{-1} for **5**, and –225±10 J K^{-1} mol^{-1} for **6**, as given in Table 3. These data lend credence to the formation of a hydrogen-bonded and well-organized transition state as presented in Fig. 9.

Reactivity of Ru(IV)-oxo complexes with different spin states

In light of the kinetic parameters listed in Tables 3 and 4, no significant difference in the reactivity was recognized among the three kinds of Ru^{IV}=O oxidants showing different spin states for the substrate oxidation reactions. Slight change in the rate constants was observed in relation to the oxidizing ability of the Ru(IV)-oxo complexes: The rate constants of **4**–**6** show linear relationships with the one-electron reduction potentials of **4**–**6** as demonstrated in Fig. 10. This observation indicates that the slight difference in the reaction rates and the activation parameters is probably derived from the difference in the electron-accepting ability of the three Ru^{IV}=O complexes,[35] but not from the difference in the spin state. Recently, Fujii and coworkers have also revealed the relationship between the activation barriers for oxidation reactions with iron-oxo complexes and the reduction potentials of the iron complexes.[38] So far, many examples have been examined to clarify the effects of difference in the spin state

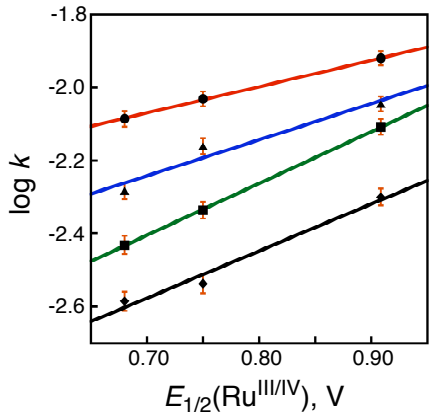

Fig. 10 Plots of log *k* for the oxidation of 1-propanol with Ru^{IV}=O complexes at various temperatures (at 308 K, filled circles and red line; at 301 K, filled triangles and blue line; at 288 K, filled squares and green line; at 280 K, filled rectangles and black line) *vs*. the one-electron reduction potentials of the Ru^{IV}=O complexes (+0.75 V for **4**, +0.68V for **5**, +0.91 V for **6**). The one-electron reduction potentials *vs*. SCE were determined for 0.05 M solutions of **4** – **6** in B.-R. buffer (pH 1.8) at room temperature.

of the metal center on the reactivity of transition-metal complexes or organometallics.[39,40] As a consequence, it has been demonstrated that the high-spin state can exhibit higher reactivity than the spin isomer at the low-spin state.[39] As recently discussed by Mayer,[41] however, the change in the reactivity may not be caused directly by the difference in the spin state, but by an indirect effect as a result of difference in $\Delta G°$ and/or reorganization energies of electron-transfer reactions. Thus, Mayer[41b] and de Visser[42] and their coworkers have indicated the important effects of the bond dissociation free-energy (BDFE) or bond dissociation enthalpy (BDE) of the metal-oxo complexes on the reactivity for the oxidation reactions.

Mechanistic insight into hydrogen atom abstraction

Three possible reaction mechanisms can be considered for the H-atom abstraction from substrates: One-step hydride transfer as a two-electron oxidation step, electron transfer followed by proton transfer (ET/PT), and concerted proton-coupled electron transfer (PCET), in which a proton and an electron are transferred in a concerted manner.[43] Hydrogen atom transfer (HAT) reactions are also defined as the simultaneous transfer of an electron and proton between the same donor and acceptor.[44] However, PCET reactions typically involve different acceptors for the electron and proton,[51] as in the present case where electron is transferred to the Ru(IV) center, but proton is transferred to the oxo ligand of Ru^{IV}=O complexes. Because there is no significant difference in the reactivity between **1** with $S = 1$ and **2** and **3** with $S = 0$, the one-step hydride transfer, which is spin-forbidden for **1** to give the product at the singlet state, is unlikely to occur. The observation of the deuterium kinetic isotope effect (*vide supra*) and the small slope of the linear correlations between log *k* and $E_{1/2}$ in Fig. 10 (0.7 at 308 K, 1.0 at 301 K, 1.4 at 288 K, and 1.3 at 280 K, respectively) indicate that the rate-determining step cannot be electron transfer. As pointed out by Hammarström and coworkers,[45] the rate constants of ET/PT should be much more sensitive to the driving forces ($\Delta G°$) of electron-transfer reaction. Thus, a concerted PCET mechanism,[46-51] which is spin-allowed and irrespective of the spin states of the Ru^{IV}=O complexes and energetically favorable, must be dominant in the oxidation of substrates with the three oxidants **4**–**6**.

Conclusion

We have synthesized a novel Ru(II)-aqua complex **3** and the corresponding Ru^{IV}=O complex **6** by using pentadentate N4Py as the auxiliary ligand and have determined the spin state of the Ru^{IV} center in **6** to be very rare $S = 0$. As suggested for **5** by DFT calculations,[20b] complex **6** could adopt a seven-coordinated structure with a solvent water molecule, and as a result, the low spin-state is energetically stabilized relative to the intermediate spin state ($S = 1$). We also employed other Ru(II)-aqua complexes **1** and **2** together with **3**, which bear similar pyridylamine coordination environments, as catalysts for oxidations of alcohols and olefins in the presence of CAN as an electron-transfer oxidant in an aqueous buffer solution to observe efficient and selective catalysis. Furthermore, the reactivity of the three analogous Ru^{IV}=O complexes **4**–**6** in oxidation reactions was also scrutinized in the light of kinetic analyses on the oxidation reactions of organic substrates. As a result, the oxidation reaction was indicated to involve a pre-equilibrium process to form adducts between the Ru(IV)-oxo complexes and substrates through hydrogen bonding for alcohols and non-covalent interactions for EBS. Based on the activation parameters of the reactions and the kinetic isotope effect on the oxidation of methanol, it was clearly indicated that the slight difference in the reaction rates can be accounted by that in the reduction potentials of the Ru^{IV}=O complexes and that the spin states of the metal centers in the Ru(IV)-oxo complexes do not influence the reactivity. It was also clarified that the H-atom abstraction from substrates proceeded *via* a concerted PCET mechanism, in which a proton and an electron are transferred simultaneously from the substrate to the Ru(IV)-oxo complexes. Substrate oxidation is one of the most important chemical processes not only for chemical industry but also for future energy production through artificial photosynthetic systems. The Ru^{IV}=O complexes presented here have exhibited one of the strongest oxidation reactivity in an energetically favorable PCET process involving a well-organized transition state. This work may provide a valuable basis to elucidate the reactivity of a high-valent metal-oxo complex in oxidation reactions of organic molecules, especially, in those involving C-H bond functionalization.

Experimental section

General

Chemicals and solvents were used as received from Tokyo Chemical Industry (TCI) Co., Wako chemicals, or Sigma-Aldrich Corp. unless otherwise mentioned. Synthetic details are described in ESI. $(NH_4)_2[Ce^{IV}(NO_3)_6]$ (CAN) was used as received and its purity was determined to be 95% by iodometry (*see* ESI). UV-vis spectra were obtained on a Shimadzu UV-3600 spectro-photometer, equipped with a UNISOK cryostat system, Unispecs. ^{1}H NMR spectra were recorded on a JEOL EX-270 spectrometer in D_2O (deuteration percentage: 99.9%) at room temperature and

the chemical shift of each signal was determined relative to DSS (4,4-dimethyl-4-silapentane-1-sulfonic acid) as an internal reference. ESI-MS spectra were recorded on a JEOL AccuTOF CS JMS-T100CS mass spectrometer. Electrochemical measurements were performed on a BAS CV-1B voltammetric analyzer and an AUTOLAB PGSTAT12 potentiometer in Britton-Robinson (B.-R.) buffer (pH = 1.8~12)[27] at room temperature with a platinum disk as a working electrode, a platinum wire as a counter electrode, and $Ag/AgNO_3$ as a reference electrode. The raw potential was converted to those relative to SCE as 0 V by adding 0.29 V. Measurements of pH values were performed on a Horiba F-51 pH-Meter. Sample solutions of **6** for resonance Raman spectroscopic measurements were prepared with a 2 mM $H_2{}^{16}O$ or $H_2{}^{18}O$ solution of **3** (50 μL), which was oxidized by addition of a 20 mM aqueous solution of CAN (20 μL).

Electrochemical generation of 4–6

A platinum mesh and a platinum wire employed as a working electrode and a counter electrode, respectively, were polished with 3M HNO_3 (aq) and rinsed well with water and dried before use. A silver wire was electrochemically oxidized in 0.1 M HCl(aq) to generate an AgCl thin layer on the surface, which reached to 1 cm high from the tip of the wire. The Ag/AgCl wire was used as a reference electrode. These three electrodes were immersed in 0.5 mM sample solutions in B.-R. buffer (2 mL) in a electrochemical vessel equipped with an optical cell of 2-mm optical path length.[27] To this electrochemical system was loaded +1.3 V (*vs*. Ag/AgCl) potentiostatic voltage for 60 min with use of an AUTOLAB PGSTAT12 potentiometer, and the process of the reaction was monitored by UV-Vis spectroscopy.

General procedures for catalytic oxidation reactions of organic substrates

A substrate (0.1 M) is dissolved in D_2O (deuteration percentage: 99.9%) in the presence of a catalyst (**1**, **2** or **3**) (1 μM) and DSS (4 mM) as an internal standard to determine the chemical shifts and also to quantify the substrate and the product. Before adding an oxidant, ^{1}H NMR spectrum of the solution was measured. After adding CAN (0.2 M) to the solution, the solution was stirred for 1 h at 23 °C and then ^{1}H NMR spectrum of the resulting solution was measured to determine the yield of the oxidation product. The catalytic oxidation of *p*-methylbenzyl alcohol with each catalyst was done for three times to check the reproducibility. For other substrates, the experiments were done for one time with each the catalyst.

Kinetic studies on oxidation reactions with Ru^{IV}=O species

The Ru^{IV}=O species, **4**, **5** and **6** (0.5 mM) were generated in B.-R. buffer (pH 1.8) from the corresponding Ru^{II}-aqua complexes **1**, **2** and **3**, respectively, through a bulk electrolysis as mentioned above. To the solution of the Ru^{IV}=O complex generated, was added substrates (1-propanol, sodium 4-ethylbenzenesulfonate, methanol and the deuterated derivatives) with various concentrations at various temperatures. The reaction profiles were monitored by the rise of the absorption assigned to the resulting Ru^{II}-OH_2 complex at 620 nm for **4**, 630 nm for **5**, and 440 nm for **6**. The error bars (drawn as hammer-shaped orange lines) in Figures for the kinetic studies and standard deviations of the kinetic and thermodynamic parameters in Tables were estimated with accuracy values of fitting curves.

Acknowledgements

This work was supported by Grants-in-Aid (Nos. 20108010, 21350035, 22245028, and 24245011), a Global COE program, "the Global Education and Research Center for Bio-Environmental Chemistry" from the Japan Society of Promotion of Science (JSPS, MEXT) of Japan, and by KOSEF/MEST through WCU project (R31-2008-000-10010-0) of Korea. T. K. also appreciates financial supports from The Asahi Glass Foundation and The Iwatani Naoji Foundation.

Notes and references

[a] *Department of Chemistry, Graduate School of Pure and Applied Sciences, University of Tsukuba, 1-1-1 Tennoudai, Tsukuba, Ibaraki 305-8571, Japan. Fax: (+) 81-29-853-6503, E-mail: kojima@chem.tsukuba.ac.jp*

[b] *Department of Material and Life Science, Graduate School of Engineering, Osaka University, ALCA, JST, 2-1 Yamada-oka, Suita, Osaka 565-0871, Japan. E-mail: fukuzumi@chem.eng.osaka-u.ac.jp*

[c] *Graduate School of Life Science, University of Hyogo, Kouto, Hyogo 678-1297, Japan.*

[d] *Department of Bioinsipired Science (WCU project), Ewha Womans University, Seoul 120-750, South Korea.*

† Electronic Supplementary Information (ESI) available: Synthetic and experimental details, UV-Vis spectral changes, MS, resonance Raman and NMR spectra are included. See DOI: 10.1039/b000000x/

1 (a) R. A. Sheldon and J. K. Kochi, *Metal-Catalyzed Oxidations of Organic Compounds*, Academic Press, New York, 1981; (b) W. A. Nugent and J. M. Mayer, *Metal-Ligand Multiple Bonds*, Wiley, New York, 1988; (c) B. Meunier, *Biomimetic Oxidations Catalyzed by Transition Metal Complexes*, Imperial College Press, London, 1998; (d) T. Punniyamurthy, S. Velusamy, J. Iqbal, *Chem. Rev.,* 2005, **105**, 2329.

2 (a) P. R. Ortiz de Montellano, *Cytochrome P450: Structure Mechanism, and Biochemistry*, 3rd ed., Kluwer Academic/Plenum, New York, 2004; (b) B. Meunier, S. P. de Visser and S. Shaik, *Chem. Rev.,* 2004, **104**, 3947; (c) I. G. Denisov, T. M. Makris, S. G. Sligar and I. Schlichting, *Chem. Rev.,* **2005**, *105,* 2253–2278.

3 (a) R. H. Holm, *Chem. Rev.,* 1987, **87**, 1401; (b) A. E. Shilov and G. B. Shul'pin, *Chem. Rev.,* 1997, **97**, 2879; (c) D. Balcells, E. Clot and O. Eisenstein, *Chem. Rev.,* 2010, **110**, 749; (d) A. Gunay and K. H. Theopold, *Chem. Rev.* 2010, **110**, 1060.

4 (a) L. Que, Jr. and R. Y. N. Ho, *Chem. Rev.,* 1996, **96**, 2607; (b) M. Costas, M. P. Mehn, M. P. Jensen and L. Que, Jr., *Chem. Rev.,* 2004, **104**, 939; (c) M. M. Abu-Omar, A. Loaiza and N. Hontzeas, *Chem. Rev.,* 2005, **105**, 2227; (d) J. A. Kovacs, *Science,* 2009, **299**, 1024.

5 (a) S. J. Lange, H. Miyake and L. Que, Jr. *J. Am. Chem. Soc.,* 1999, **121**, 6330; (b) N. Lehnert, R. Y. N. Ho, L. Que, Jr. and E. I. Solomon, *J. Am. Chem. Soc.*, 2001, **123**, 8271; (c) J. Kaizer, E. J. Klinker, N. Y. Oh, J.-U. Rohde, W. J. Song, A. Stubna, J. Kim, E. Münck, W. Nam and L. Que, Jr., *J. Am. Chem. Soc.,* 2004, **126**, 472; d) Y. Morimoto, H. Kotani, J. Park, Y.-M. Lee, W. Nam and S. Fukuzumi, *J. Am. Chem. Soc.,* 2011, **133**, 403; (e) J. Park, Y. Morimoto, Y.-M. Lee, W. Nam and S. Fukuzumi, *J. Am. Chem. Soc.,* 2011, **133**, 5236; (f) J. Park, Y. Morimoto, Y.-M. Lee, W. Nam and S. Fukuzumi, *J. Am. Chem. Soc*., 2012, **134**, 3903.

6 (a) J.-U. Rohde, J.-H. In, M. H. Lim, W. W. Brennessel, M. R. Bukowski, A. Stubna, E. Münck, W. Nam and L. Que, Jr., *Science,* 2003, *299*, 1037; (b) C. E. MacBeth, R. Gupta, K. R. Mitchell-Koch, V. G. Young, Jr., G. H. Lushington, W. H. Thompson, M. P. Hendrich and A. S. Borovik, *J. Am. Chem. Soc.,* 2004, **126**, 2556; c) S. Fukuzumi, Y. Morimoto, H. Kotani, P. Naumov, Y.-M. Lee and W. Nam, *Nat. Chem.,* 2010, **2**, 756; (d) D. C. Lacy, R. Gupta, K. L. Stone, J. Greaves, J. W. Ziller, M. P. Hendrich and A. S. Borovik, *J. Am. Chem. Soc.*, 2010, **132**, 12188.

7 (a) Z. Shirin, B. S. Hammes, V. G. Young, Jr. and A. S. Borovik, *J. Am. Chem. Soc.,* 2000, **122**, 1836; (b) G. Yin, M. Buchalova, A. M.

Danby, C. M. Perkins, D. Kitko, J. D. Carter, W. M. Scheper and D. H. Busch, *J. Am. Chem. Soc.,* 2005, **127**, 17170; (c) G. Yin, A. M. Danby, D. Kitko, J. D. Carter, W. M. Scheper and D. H. Busch, *J. Am. Chem. Soc.,* 2008, **130**, 16245; (d) S. Fukuzumi, N. Fujioka, H. Kotani, K. Ohkubo, Y.-M. Lee and W. Nam, *J. Am. Chem. Soc.,* 2009, **131**, 17127; (e) S. H. Kim, H. Park, M. S. Seo, M. Kubo, T. Ogura, J. Klajn, D. T. Gryko, J. S. Valentine and W. Nam, *J. Am. Chem. Soc.,* 2010, **132**, 14030.

8 J. D. Blakemore, N. D. Schley, D. Balcells, J. F. Hull, G. W. Olack, C. D. Incarvito, O. Eisenstein, G. W. Brudvig and R. H. Crabtree, *J. Am. Chem. Soc.*, *2010*, **132**, 16017.

9 T. M. Anderson, W. A. Neiwert, M. L. Kirk, P. M. B. Piccoli, A. J. Schultz, T. F. Koetzle, D. G. Musaev, K. Morokuma, R. Cao and C. L. Hill, *Science,* 2004, **306**, 2074.

10 (a) B. T. Farrer, J. S. Pickett and H. H. Thorp, *J. Am. Chem. Soc.*, 2000, **122**, 549; (b) W. W. Y. Lam, W.-L. Man, C.-F. Leung, C.-Y. Wong and T.-C. Lau, *J. Am. Chem. Soc.,* 2007, **129**, 13646.

11 (a) M. H. V. Huynh and T. J. Meyer, *Chem. Rev.,* 2007, **107**, 5004; (b) V. R. I. Kaila, M. Verkhovsky and M. Wikström, *Chem. Rev.,* 2010*,* **110***,* 7062; (c) J. J. Warren, T. A. Tronic and J. M. Mayer, *Chem. Rev.,* 2010, **110**, 6961; (d) C. J. Gagliardi, B. C. Westlake, C. A. Kent, J. J. Paul, J. M. Papanikolas and T. J. Meyer, *Coord. Chem. Rev.,* 2010, **254**, 2459.

12 (a) H. Kotani, T. Suenobu, Y.-M. Lee, W. Nam and S. Fukuzumi, *J. Am. Chem. Soc.,* 2011, **133**, 3249; b) S. Fukuzumi, T. Kishi, H. Kotani, Y.-M. Lee and W. Nam, *Nat. Chem*., 2011, **3**, 38.

13 (a) W. Rüttinger and G. C. Dismukes, *Chem. Rev.,* 1997, **97**, 1; (b) J. P. McEvoy and G. W. Brudvig, *Chem. Rev.*, 2006, **106**, 4455; (c) T. J. Meyer, M. H. V. Huynh and H. H. Thorp, *Angew. Chem., Int. Ed.,* 2007, **46**, 5284.

14 (a) K. N. Ferreira, T. M. Iverson, K. Maghlaoui, J. Barber and S. Iwata, *Science,* 2004, **303**, 1831; (b) Y. Umena, K. Kawakami, J.-R. Shen and N. Kamiya, *Nature,* 2011, **473**, 55.

15 (a) M. S. Thompson and T. J. Meyer, *J. Am. Chem. Soc.,* 1982, **104**, 4106; (b) R. A. Binstead, M. E. McGuire, A. Dovletoglou, W. K. Seok, L. E. Roecker and T. J. Meyer, *J. Am. Chem. Soc.,* 1992, **114**, 173; (c) E. L. Lebeau and T. J. Meyer, *Inorg. Chem.,* 1999, **38**, 2174; (d) R. A. Binstead, C. W. Chronister, J. Ni, C. M. Hartshorn and T. J. Meyer, *J. Am. Chem. Soc.,* 2000, **122**, 8464; (e) J. J. Concepcion, M.-K. Tsai, J. T. Muckerman and T. J. Meyer, *J. Am. Chem. Soc*., 2010, **132**, 1545.

16 (a) A. Sartorel, P. Miró, E. Salvadori, S. Romain, M. Carraro, G. Scorrano, M. Di Valentin, A. Llobet, C. Bo and M. Bonchio, *J. Am. Chem. Soc.,* 2009, **131**, 16051; (b) A. Sartorel, M. Carraro, G. Scorrano, R. De Zorzi, S. Geremia, N. D. McDaniel, S. Bernhard and M. Bonchio, *J. Am. Chem. Soc*., 2008, **130**, 5006; (c) M. Murakami, D. Hong, T. Suenobu, S. Yamaguchi, T. Ogura and S. Fukuzumi, *J. Am. Chem. Soc*., 2011, **133**, 11605.

17 (a) Y. V. Geletii, C. Besson, Y. Hou, Q. Yin, D. G. Musaev, D. Quiñonero, R. Cao, K. I. Hardcastle, A. Proust, P. Kögerler and C. L. Hill, *J. Am. Chem. Soc*., 2009, **131**, 17360; (b) A. E. Kuznetsov, Y. V. Geletii, C. L. Hill, K. Morokuma and D. G. Musaev, *J. Am. Chem. Soc*., 2009, **131**, 6844; (c) Y. V. Geletii, B. Botar, P. Kögerler, D. A. Hillesheim, D. G. Musaev and C. L. Hill, *Angew. Chem., Int. Ed*., 2008, **47**, 3896.

18 (a) F. Bozoglian, S. Romain, M. Z. Ertem, T. K. Todorova, C. Sens, J. Mola, M. Rodríguez, I. Romero, J. Benet-Buchholz, X. Fontrodona, C. J. Cramer, L. Gagliardi and A. Llobet, *J. Am. Chem. Soc.,* 2009, **131**, 15176; (b) S. Romain, F. Bozoglian, X. Sala and A. Llobet, *J. Am. Chem. Soc*., 2009, **131**, 2768.

19 (a) W. K. Seok and T. J. Meyer, *J. Am. Chem. Soc.,* 1988, **110**, 7358; (b) A. Paul, J. F. Hull, M. R. Norris, Z. Chen, D. H. Ess, J. J. Concepcion and T. J. Meyer, *Inorg. Chem.,* 2011, **50**, 1167.

20 (a) Y. Hirai, T. Kojima, Y. Mizutani, Y. Shiota, K. Yoshizawa and S. Fukuzumi, *Angew. Chem., Int. Ed.,* 2008, **47**, 5772; (b) T. Kojima, Y. Hirai, T. Ishizuka, Y. Shiota, K. Yoshizawa, K. Ikemura, T. Ogura and S. Fukuzumi, *Angew. Chem., Int. Ed.,* 2010, **49**, 8449.

21 (a) D. Schröder and S. Shaik, *Angew. Chem., Int. Ed.,* 2011, **50**, 3850; (b) T. Kojima and S. Fukuzumi, *Angew. Chem., Int. Ed.,* 2011, **50**, 3852.

22 M. Lubben, A. Meetsma, E. C. Wilkinson, B. Feringa and L. Que, Jr., *Angew. Chem., Int. Ed. Engl.* 1995, **34**, 1512.

23 (a) K. Shiren, S. Ogo, S. Fujinami, H. Hayashi, M. Suzuki, A. Uehara, Y. Watanabe and Y. Moro-oka, *J. Am. Chem. Soc.,* 2000, **122**, 254; (b) H. Hayashi, K. Uozumi, S. Fujinami, S. Nagatomo, K. Shiren, H. Furutachi, M. Suzuki, A. Uehara and T. Kitagawa, *Chem. Lett.,* 2002, 416; (c) D. G. Lonnon, D. C. Craig, S. B. Colbran, *Inorg. Chem. Commun.,* 2003, **6***,* 1351; (d) M. Mizuno, K. Honda, J. Cho, H. Furutachi, T. Tosha, T. Matsumoto, S. Fujinami, T. Kitagawa and M. Suzuki, *Angew. Chem., Int. Ed.* 2006, **45**, 6911.

24 T. Kojima, D. M. Weber and C. T. Choma, *Acta Cryst.* 2005, **E61**, m226.

25 A. G. Orpen, L. Brammer, F. A. Allen, O. Kennard and D. G. Watson, *J. Chem. Soc., Dalton Trans.,* 1989, S1.

26 (a) J. Benet-Buchholz, P. Comba, A. Llobet, S. Roeser, P. Vadivelu, H. Wadepohl and S. Wiesner, *Dalton Trans.,* 2009, 5910; (b) R. Zong, F. Naud, C. Segal, J. Burke, F. Wu and R. Thummel, *Inorg. Chem.,* 2004, **43**, 6195; (c) X.-J. Yang, F. Drepper, B. Wu, W.-H. Sun, W. Haehnel and C. Janiak, *Dalton Trans.,* 2005, 256; (d) N. Gupta, N. Grover, G. A. Neyhart, W. Liang, P. Singh and H. H. Thorp, *Angew. Chem., Int. Ed. Engl.,* 1992, **31**, 1048.

27 R. Wang, J. G. Vos, R. H. Schmehl and R. Hage, *J. Am. Chem. Soc*., 1992, **114**, 1964.

28 In this experiment, the aqua-complex **3** was dissolved in 99%-enriched $H_2{}^{18}O$ and then oxidized with CAN into **6**, but as the substitution rate of the aqua ligand in **3** was slow, thus the enriched efficiency of **6** observed with ESI MS spectrum was about 50%.

29 The Raman scatterings derived from the Ru^{IV}=O moiety in **6** and the ^{18}O-derivative were very weak, because the Ru(IV)-oxo complex underwent facile photo-conversion to afford the corresponding aqua-complex **3** by the laser excitation at 353 nm. Details of the photo-conversion are currently under investigation.

30 T. Kojima, K. Nakayama, K. Ikemura, T. Ogura and S. Fukuzumi, *J. Am. Chem. Soc.,* 2011, **133**, 11692.

31 In this experiment, 10 mol equiv of CAN was required despite that the theoretical requirement was only 2 mol equiv. The reason may result from the relation between the stability of CAN and the solution pH. In fact, UV-Vis experiments indicated that 10 mol equiv CAN was required to fully oxidize **3** into **6** in neutral water, whereas the reaction was completed with addition of 2 mol eq of CAN in B.-R. buffer (pH 1.8) (Fig. S8 in ESI).

32 The assignment of the ^{1}H NMR signals of the pyridine rings was made by a differential NOE spectrum of complex **6** in D_2O. The signal due to 3-H of the N2- and N3-pyridine rings at 9.00 ppm showed a correlation with the signal assigned to the methine proton at 7.41 ppm (Fig. S10 in ESI).

33 Experimental details of the controlled experiments are described in ESI and the ^{1}H NMR spectra of the selected examples for the oxidation reaction of the substrates with CAN only are shown in Fig. S12 in ESI with the oxidation efficiencies. See ESI.

34 Y.-R. Luo, *Handbook of Bond Dissociation Energies in Organic Compounds, Boca Raton*, CRC Press, 2003.

35 (a) E. A. Mader, E. R. Davidson and J. M. Mayer, *J. Am. Chem. Soc.,* 2007, **129**, 5153; (b) W.W. Y. Lam, M. F. W. Lee and T.-C. Lau, *Inorg. Chem.,* 2006, **45**, 315.

36 The obtained rate constants and the activation parameters for **4** and **5** are slightly different from those reported in previous reports (ref. 20b). Probably the reason is ascribed to the difference in the generation methods of the oxo species. In ref. 20b, the oxo complexes as active species were formed with addition of 2 mol eq of CAN in neutral water.

37 (a) I. Garcia-Bosch, A. Company, C. W. Cady, S. Styring, W. R. Browne, X. Ribas and M. Costas, *Angew. Chem., Int. Ed.,* 2011, **50**, 5648; (b) T. Steiner, *Angew. Chem., Int. Ed.,* 2002, **41**, 48.

38 A. Takahashi, D. Yamaki, K. Ikemura, T. Kurahashi, T. Ogura, M. Hada and H. Fujii, *Inorg. Chem.* 2012, **51**, 7296.

39 (a) H. Hirao, D. Kumar, L. Que, Jr. and S. Shaik, *J. Am. Chem. Soc.,* 2006, **128**, 8590; (b) S. N. Dhuri, M. S. Seo, Y.-M. Lee, H. Hirao, Y. Wang, W. Nam and S. Shaik, *Angew. Chem., Int. Ed.,* 2008, **47**, 3356; (c) E. J. Klinker, S. Shaik, H. Hirao and L. Que, Jr., *Angew. Chem., Int. Ed.,* 2009, **48**, 1291; (d) G. Q. Xue, R. De

Hont, E. Munck and L. Que, Jr., *Nat. Chem.,* 2010, **2**, 400; (e) D. Janardanan, Y. Wang, P. Schyman, L. Que, Jr. and S. Shaik, *Angew. Chem., Int. Ed.* 2010, **49**, 3342; (f) M. S. Seo, N. H. Kim, K.-B. Cho, J. E. So, S. K. Park, M. Clemancey, R. Garcia-Serres, J.-M. Latour, S. Shaik and W. Nam, *Chem. Sci.,* 2011, **2**, 1039.

40 (a) J. L. Detrich, O. M. Reinaud, A. L. Rheingold, and K. H. Theopold, *J. Am. Chem. Soc.,* 1995, **117**, 11745; (b) D. W. Keogh and R. Poli, *J. Am. Chem. Soc.,* 1997, **119**, 2516; (c) J. L. Carreón-Macedo and J. N. Harvey, *J. Am. Chem. Soc.,* 2004, **126**, 5789; (d) J. N. Harvey, P. Poli and K. M. Smith, *Coord. Chem. Rev.,* 2003, **238**, 347; (e) N. A. Eckert, S. Vaddadi, S. Stoian, R. J. Lachicotte, T. R. Cundari and P. L. Holland, *Angew. Chem., Int. Ed.,* 2006, **45**, 6868.

41 (a) J. C. Yoder, J. P. Roth, E. M. Gussenhoven, A. S. Larsen and J. M. Mayer, *J. Am. Chem. Soc.,* 2003, **125**, 2629. (b) J. M. Mayer, *Acc. Chem. Res.,* 2011, **44**, 36.

42 D. Kumar, B. Karamzadeh, G. N. Sastry and S. P. de Visser, *J. Am. Chem. Soc.*, 2010, **132**, 7656.

43 For the mechanistic border line between ET/PT and concerted PCET, see: (a) J. Yuasa and S. Fukuzumi, *J. Am. Chem. Soc.,* 2006, **128**, 14281; (b) S. Fukuzumi and H. Kotani, in *Proton-Coupled Electron Transfer*, RSC Catalysis Series No. 8 (ed. S. Formoshinho, M. Barroso), RSC Publishing, Cambridge, Wilkinson), 2012, pp. 89-125.

44 A. Sirjoosingh and S. Hammes-Schiffer, *J. Phys. Chem. A,* 2011, **115**, 2367.

45 (a) M. Sjödin, S. Styring, H. Wolpher, Y. Xu, L. Sun and L. Hammarström, *J. Am. Chem. Soc.,* 2005, **127**, 3855; (b) A. A. Zieba, C. Richardson, C. Lucero, S. D. Dieng, Y. M. Gindt and J. P. M. Schelvis, *J. Am. Chem. Soc.,* 2011, 133, 7824.

46 E. A. Mader and J. M. Mayer, *Inorg. Chem.,* 2010, **49**, 3685.

47 (a) M. J. Knapp, K. W. Rickert and J. P. Klinman, *J. Am. Chem. Soc.,* 2002, **124**, 3865; (b) E. Hatcher, A. V. Soudackov and S. Hammes-Schiffer, *J. Am. Chem. Soc.,* 2007, **129**, 187; (c) M. P. Meyer and J. P. Klinman, *Chem. Phys.,* 2005, **319**, 283; (d) M. K. Ludlow, A. V. Soudackov and S. Hammes-Schiffer, *J. Am. Chem. Soc.,* 2009, **131**, 7094.

48 C. J. Fecenko, H. H. Thorp and T. J. Meyer, *J. Am. Chem. Soc.,* 2007, **129**, 15098.

49 (a) M. Sjödin, S. Styring, B. Åkermark, L. Sun and L. Hammarström, *J. Am. Chem. Soc.,* 2000, **122**, 3932; (b) M. K. Ludlow, A. V. Soudackov and S. Hammes-Schiffer, *J. Am. Chem. Soc.,* 2009, **131**, 7094.

50 (a) R. A. Binstead, M. F. McGuire, A. Dovletglou, W. K. Seok, L. E. Roecker and T. J. Meyer, *J. Am. Chem. Soc.,* 1992, **114**, 173; (b) E. L. Lebeau, R. A. Binstead and T. J. Meyer, *J. Am. Chem. Soc.,* 2001, **123**, 10535; (c) M. H. V. Huynh and T. J. Meyer, *Angew. Chem., Int. Ed.,* 2002, **41**, 1395.

51 S. Hammes-Schiffer, *Acc. Chem. Res.,* 2009, **42**, 1881.